Effects of crack size distribution and specimen length on the correlation between n-value and critical current in heterogeneously cracked superconducting tape

AUTHOR(S):

Ochiai, Shojiro; Okuda, Hiroshi; Fujii, Noriyuki

CITATION:

Ochiai, Shojiro ...[et al]. Effects of crack size distribution and specimen length on the correlation between n-value and critical current in heterogeneously cracked superconducting tape. Materials Transactions 2017, 58: 1469-1478

ISSUE DATE:

2017-10-01

URL:

http://hdl.handle.net/2433/250426

Materials Transactions, Vol. 58, No. 10 (2017) pp. 1469 to 1478

Effects of Crack Size Distribution and Specimen Length on the Correlation between *n*-Value and Critical Current in Heterogeneously Cracked Superconducting Tape

Shojiro Ochiai[1], Hiroshi Okuda[2] and Noriyuki Fujii[2,*]

[1]*Elements Strategy Initiative for Structural Materials, Kyoto University, Kyoto 606–8501, Japan*
[2]*Department of Materials Science and Engineering, Kyoto University, Kyoto 606–8501, Japan*

A Monte Carlo simulation study was carried out to reveal the effects of crack size distribution and specimen length on the correlation between *n*-value and critical current in heterogeneously cracked superconducting tapes. First, it was shown that, with increasing distribution width of crack size, the distribution widths of critical current and *n*-values increase, and, the average critical current-value and average *n*-value of specimens decrease. Also, it was shown that the decrease in average *n*-value with increase in distribution width of crack size is more intense than the decrease in average critical current-value and this feature is more pronounced in longer specimens. Then it was revealed that plural *n*-values can exist for one critical current value since the *n*-value of specimen was dependent on the positional relation among the voltage-current curves of the sections, of which specimen is constituted. This phenomenon could be described by the difference in the resistance value in the current shunting circuit by application of a single equivalent crack-current shunting model in which the cracks within a specimen are replaced by a single equivalent crack. Based on this result, an approach, in which the resistance value in the current shunting circuit is used to describe the upper-lower bounds and the center of *n*-value in the correlation diagram between *n*-value and critical current, was presented. It was shown that the correlation diagrams at various distribution widths of crack size and specimen lengths, obtained by simulation and experiments, are described well by this approach. [doi:10.2320/matertrans.MAW201702]

(Received March 29, 2017; Accepted May 19, 2017; Published June 16, 2017)

Keywords: *superconducting tape, heterogeneous cracking, Monte Carlo simulation, specimen length, critical current, n-value*

1. Introduction

Two types of superconducting tapes have been developed. One is the superconducting layer RE(Y, Sm, Dy, Gd, ...)$Ba_2Cu_3O_{7-\delta}$ -coated tapes (hereafter, noted as coated conductor tapes). Another is the superconducting filaments $Bi_2Sr_2Ca_2Cu_3O_{10+x}$, Nb_3Sn, Nb_3Al and MgB_2-embedded tapes (filamentary conductor tapes). Both coated- and filamentary- conductor tapes are subjected to thermal, mechanical and electromagnetic stresses/strains during fabrication and operation. When the superconducting layers/filaments are cracked by such stresses, the critical current I_c and *n*-value both of coated[1–10] and filamentary[11–19] conductor tapes are reduced. In ordinary cases, cracking of the coated layer/filament takes place heterogeneously. As a specimen is composed of a series electric circuit of local sections, the I_c and *n*-value of sections within a specimen are different to each other, and the I_c and *n*-value of a specimen depends on the extent of cracking in sections[5,8,11,15].

If cracking takes place homogeneously, all sections have the same I_c and same *n*-value and the specimen constituted of the sections has also the same I_c and same *n*-value as those of the sections. Namely, in the virtual case of completely homogeneous cracking, the I_c and *n*-value do not vary with specimen length. On the other hand, in the practical case of heterogeneous cracking, the I_c and *n*-value of specimen tends to decrease with increasing specimen length, as has been observed experimentally for $SmBa_2Cu_3O_{7-\delta}$ -coated tape[8] and $Bi_2Sr_2Ca_2Cu_3O_{10+x}$ filamentary tape[15].

In experimental work, it is difficult to control artificially the crack size distribution. A new approach is required to obtain systematically the information on the role of crack size distribution and specimen length in determination of I_c and *n*-value. In our recent work[20], we applied a Monte Carlo simulation method combined with a current shunting model at cracks[13] to reveal systematically the effects of crack size distribution on I_c and *n*-value for various specimen lengths under a fixed average crack size. With this approach, how the distributions of I_c and *n*-value vary with varying distribution width of crack size and specimen length could be monitored[20]. In the present work, this approach was extensively applied to a wide range of crack size to investigate the effects of crack size distribution and specimen length on the correlation between I_c and *n*-value in heterogeneously cracked superconducting tapes.

2. Procedure of Simulation

2.1 Model of specimen and model of current shunting at a crack

Figure 1(a)[20] shows the configuration of the model specimen. The specimen is constituted of a series electric circuit of N sections (S(1), S(2),...S(N)) with a length L_0 = 1.5 cm. Each of N sections has one crack. The crack size is different from section to section. N was varied from 1 to 20 and accordingly the length of the specimen $L = NL_0$ was varied from 1.5 to 30 cm.

For description of the *V*–*I* relation of sections under an existent partial crack, the model of Fang *et al.*[13] was employed in a modified form as in our works[3–5,8–10,14,15,20,21], where partial crack means the crack that exists in a part of transverse cross-section of the superconducting phase. The part where crack is not extended in the cracked cross-section is named as a ligament part. Current path in a section with a crack is shown schematically in Fig. 1(b)[8], in which one section in coated tape specimen is representatively drawn. Noting the I_c- and *n*-values of sections without crack as I_{c0} and n_0, respectively, the critical electric field for determina-

[*]Graduate Student, Kyoto Univerasity

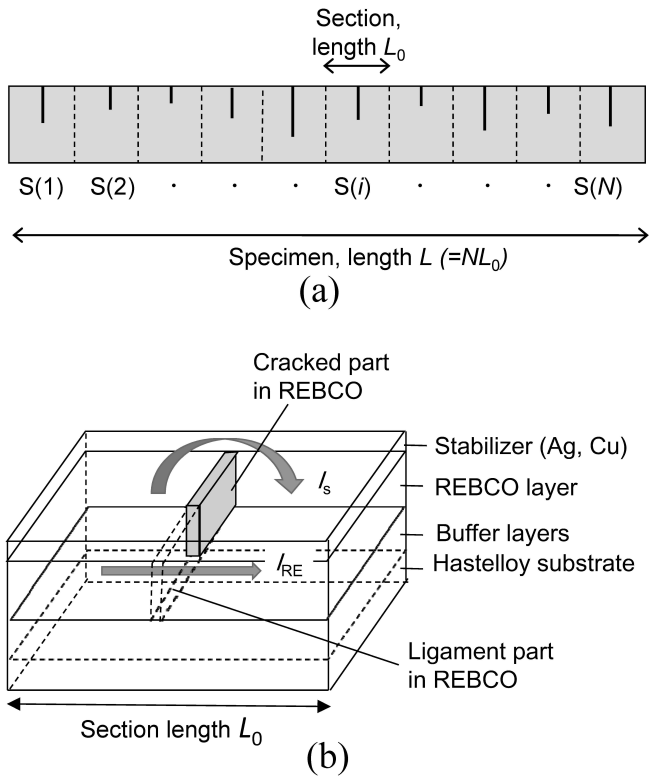

Fig. 1 Schematic representation of (a) the model specimen with length L (3~30 cm), composed of a series of sections with a length L_0 (= 1.5 cm in this work) and (b) current path in a section with a partial crack, taken from our preceding work[20].

tion of critical current as E_c (= 1 μV/cm), the relative crack size (= the ratio of the area of cracked part to the total cross-sectional area of the superconducting layer) and the relative ligament size (= ratio of the area of the ligament part to the total cross-sectional area of the superconducting layer) as f and $1 - f$, respectively, the current transported by the ligament part as I_{RE}, the shunting current at the cracked part as I_s, the electric resistance in shunting circuit as R_t, the voltages developed in the ligament part and in the cracked part as V_{RE} and V_s ($= V_{RE}$ since the ligament- and cracked parts constitute of a parallel circuit), respectively, and the current transfer length as s ($<<L_0$)[9,10], we can express the V–I relation of the section (L_0 = 1.5 cm) without crack by eq. (1) and that with a crack by eqs. (2) and (3)[3–5,8,14,15],

$$V = E_c L_0 \left(\frac{I}{I_{c0}}\right)^{n_0} \tag{1}$$

$$V = E_c L_0 \left(\frac{I}{I_{c0}}\right)^{n_0} + V_{RE} \tag{2}$$

$$I = I_{RE} + I_s = I_{c0}(1-f)\left(\frac{L_0}{s}\right)^{1/n_0}\left[\frac{V_{RE}}{E_c L_0}\right]^{1/n_0} + \frac{V_{RE}}{R_t} \tag{3}$$

The term $(1 - f)(L_0/s)^{1/n_0}$ in eq. (3) is, hereafter, noted as the ligament parameter $L_{p,section}$. This parameter was derived by the authors[3,4,8,9,14] by modifying the formulation of Fang *et al.*[13] The $L_{p,section}$ has a physical meaning as I_c/I_{c0} (the ratio of critical current in cracked state (I_c) to the critical current in non-cracked state (I_{c0})) in the case where the voltage V_{RE} developed at crack is equal to the whole voltage V and shunting current is negligible[9,10,15]. In practice, current shunting occurs and voltage is developed not only at cracks but also at the non-cracked area away from the crack. Hence the I_c/I_{c0} is not equal to the ligament parameter in practical tapes. However, it is noted that the ligament parameter still gives a fairly good approximation for I_c/I_{c0}, as has been shown in our former works for coated[3–5,8,9] and filamentary[14,15] tapes. In this work, the ligament parameter $L_{p,section}$, which is proportional to the relative ligament size $1 - f$ where f is the relative crack size, was used as a monitor of crack size (the larger the ligament parameter, the smaller is the crack size) similarly to the preceding works[10,15,20,21].

2.2 Monte Carlo simulation of V–I curve, I_c and n-value of sections and specimens

The standard deviation of $1 - f$ is equal to that of f. Wide/narrow distribution of ligament size ($1 - f$) corresponds to wide/narrow distribution of crack size (f). As a monitor of the distribution width of crack size, the standard deviation of the ligament parameter $\Delta L_{p,section}$ was used as in our preceding work[20]. For formulation of distribution of values of $L_{p,section}$ of cracked sections with a length L_0, the normal distribution function was used. Noting the average of $L_{p,section}$ as $L_{p,section,ave}$, the cumulative probability $F(L_{p,section})$ was expressed by

$$F(L_{p,section}) = \frac{1}{2}\left\{1 + \mathrm{erf}\left(\frac{L_{p,section} - L_{p,section,ave}}{\sqrt{2}\Delta L_{p,section}}\right)\right\} \tag{4}$$

In this work, $L_{p,section,ave}$ was given to be 0.400, 0.670 and 0.940, corresponding to large, intermediate and small average crack size, respectively. $\Delta L_{p,section}$ was given to be 0.05 and 0.15, corresponding to narrow and wide distribution of crack size, respectively. The $L_{p,section}$ was given to each cracked section with a Monte Carlo method by generating a random value R (= 0~1), setting $F(L_{p,section}) = R$ in eq. (4), and substituting the aforementioned values of $L_{p,section,ave}$ and $\Delta L_{p,section}$ in eq. (4).

The V–I curve of each cracked section with a length L_0 = 1.5 cm was calculated by substituting the $L_{p,section}$-value given by the Monte Carlo procedure stated above, R_t = 2 $\mu\Omega$, which was an average value obtained by analysis of the V–I curves of cracked DyBCO conductor tapes with a length L_0 = 1.5 cm, measured at 77 K in a self-magnetic field under applied tensile stresses[5], into eqs. (2) and (3). The I_c and n-value in the non-cracked state were given by I_{c0} = 200 A and n_0 = 40, respectively. The simulation procedure was repeated for 120 times, and 120 sets of V–I curve of sections were obtained for each combination of $L_{p,section,ave}$ value (0.400, 0.670, 0.940) with $\Delta L_{p,section}$ value (0.05, 0.15).

As the specimen is constituted of a series electric circuit of sections (Fig. 1(a)), the current I of the specimen and all sections is the same;

$$I = I_{S(i)} \quad (i = 1 \text{ to } N) \tag{5}$$

The voltage V of specimen is the sum of the voltages of all sections

$$V = \sum_{i=1}^{N} V_{S(i)} \tag{6}$$

Using the *V–I* curves of the sections (L_0 = 1.5 cm), we calculated the *V–I* curves of the specimens with eqs. (5) and (6) for L = 3 to 30 cm, corresponding to N = 2 to 20. From the obtained *V–I* curves, the I_c-values of the sections and specimens were obtained as a value of I at $E = E_c$ = 1 μV/cm (corresponding to $V = V_c = E_c L$ μV). The *n*-values of the sections and specimens were obtained by fitting the *E–I* curve to the form of $E \propto I^n$ for the electric field range of E = 0.1~10 μV/cm, namely by fitting the *V–I* curve to the form of $V \propto I^n$ for the voltage range of $V = 0.1L$~$10L$ μV.

3. Results and Discussion

3.1 Effects of average crack size, crack size distribution and specimen length on critical current and *n*-value

Figure 2 shows simulated I_c- and *n*-values of specimens (shown with open circles) and their average values, $I_{c,ave}$ and n_{ave}, (shown with open rectangles), plotted against the average ligament parameter of sections $L_{p.section,ave}$. In this example, the results of the specimens with a length L = 7.5 cm were taken up representatively. (a, a') and (b, b') show the simulation results of I_c- and *n*-values, under the condition of $\Delta L_{p,section}$ = 0.05 and 0.15, respectively.

Important features are read from the results in Fig. 2. (i) Comparing (a) with (a') and comparing (b) with (b'), the larger the value of $\Delta L_{p,section}$; namely, the larger the difference in ligament size (= the larger the difference in crack size) among the sections, the wider became the distribution of both I_c- and *n*-values of specimens and the lower became the $I_{c,ave}$- and n_{ave}-values of specimens. (ii) The values of $I_{c,ave}/I_{c0}$ in (a, b) and n_{ave}/n_0 in (a', b') refer to the normalized average critical current and *n*-value with respect to the original values I_{c0} and n_0 in non-cracked state, respectively. Comparing the n_{ave}/n_0 in (a') and (b') with $I_{c,ave}/I_{c0}$ in (a) and (b), respectively, n_{ave}/n_0 was lower than $I_{c,ave}/I_{c0}$ at any $L_{p,section,ave}$, namely at any average crack size. This means that *n*-value was reduced by cracking more severely than I_c-value.

Figure 3 shows (a, b) $I_{c,ave}$ and (a',b') n_{ave}, obtained for $L_{p,section,ave}$ = 0.400, 0.670 and 0.940 under the condition of $\Delta L_{p,section}$ = (a, a') 0.05 and (b, b') 0.15, plotted against specimen length L. The following features were found.

(1) For any specimen length L and for any standard deviation of ligament parameter of sections $\Delta L_{p,section}$, the $I_{c,ave}$ and n_{ave} decreased with decreasing average ligament parameter of sections, $L_{p,section,ave}$, namely with increasing average crack size, as expected.

(2) For any values of $L_{p,section,ave}$ and $\Delta L_{p,section}$; namely for any average crack size and any distribution width of crack size, both of $I_{c,ave}$ and n_{ave} decreased significantly and then gradually with increasing specimen length L.

(3) The decrease in $I_{c,ave}$ with increasing L was small when $\Delta L_{p,section}$ was small (= when the distribution width of crack size was small) as shown in (a), but it was large when

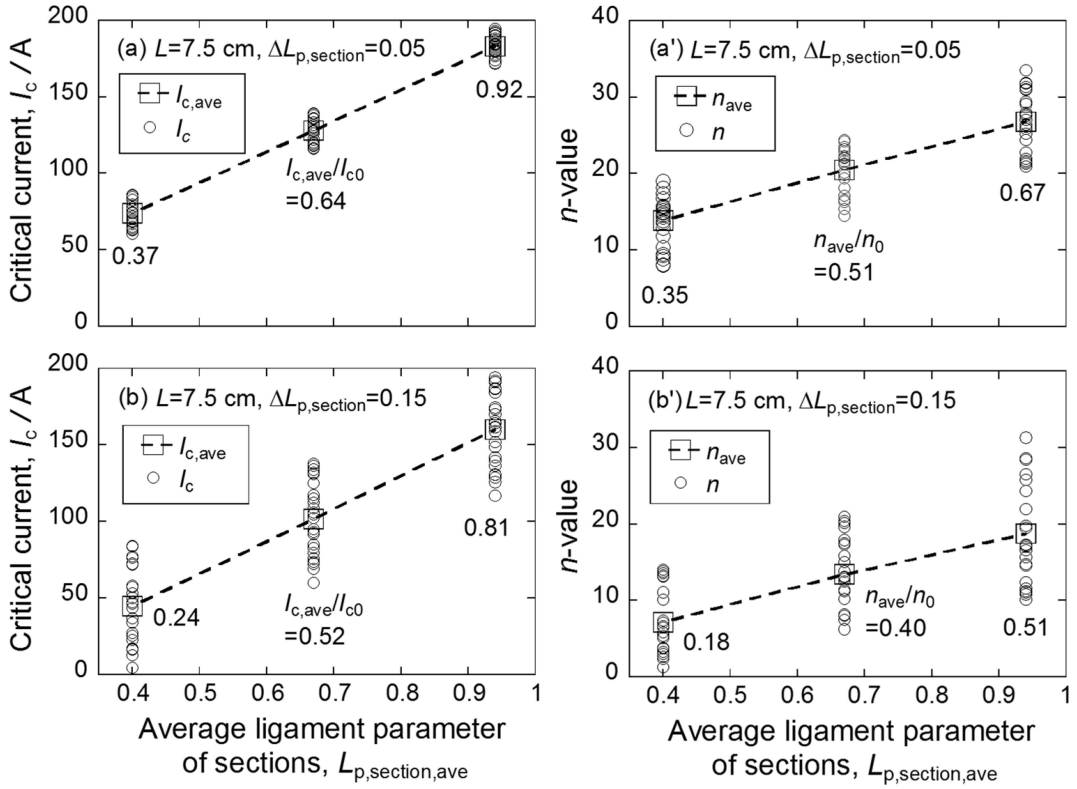

Fig. 2 Critical current I_c, *n*-value and their average values ($I_{c,ave}$ and n_{ave}) of the specimens simulated for average ligament parameter of sections $L_{p.section,ave}$ = 0.400, 0.670 and 0.940, and standard deviation of the ligament parameter of the sections $\Delta L_{p,section}$ = 0.05 and 0.15. The results of the specimens with a length L = 7.5 cm are taken up representatively. (a) and (b) refer to the results of critical current for $\Delta L_{p,section}$ = 0.05 and 0.15, respectively, and (a') and (b') refer to the results of *n*-value for $\Delta L_{p,section}$ = 0.05 and 0.15, respectively. The $I_{c,ave}/I_{c0}$ and n_{ave}/n_0 refer to the normalized average critical current and *n*-value with respect to the original values I_{c0} and n_0, respectively.

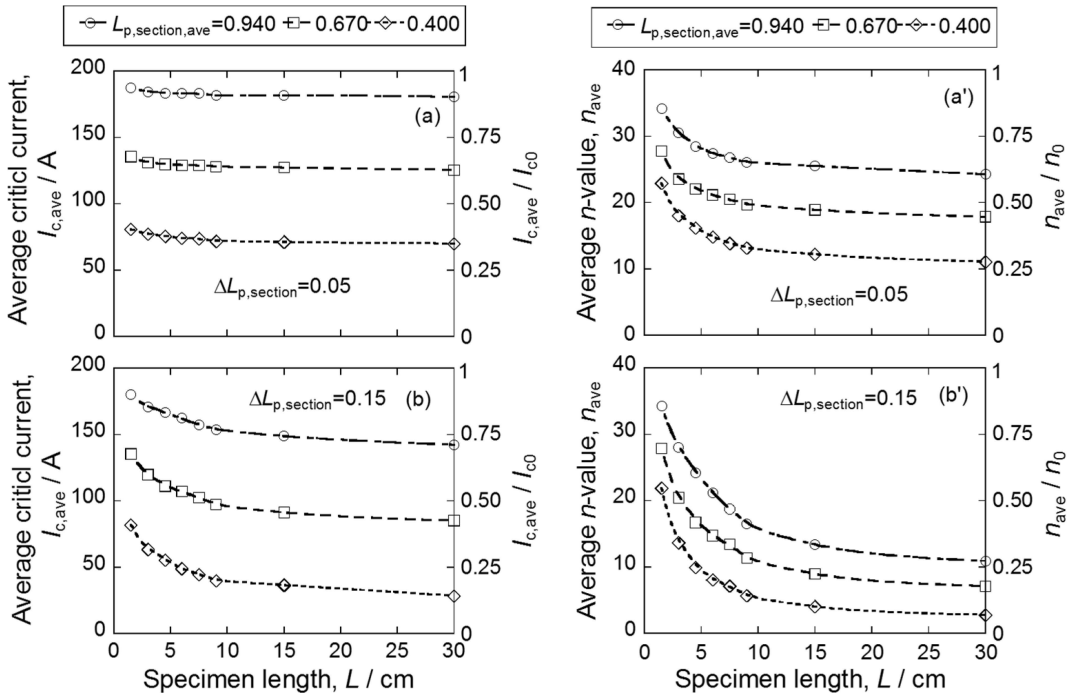

Fig. 3 Simulated average values of (a, b) critical current, $I_{c,ave}$, and (a', b') n-value, n_{ave}, for $L_{p,section,ave}$ = 0.940, 0.670 and 0.400 and for standard deviation of the ligament parameter of sections $\Delta L_{p,section}$ = (a, a') 0.05 and (b, b') 0.15, plotted against sample length L. For reference, the $I_{c,ave}$ normalized with respect to I_{c0}, $I_{c,ave}/I_{c0}$ and the n_{ave} normalized with respect to n_0, n_{ave}/n_0, are shown in the right axis in (a, b) and (a', b'), respectively.

$\Delta L_{p,section}$ was large (= when the distribution width of crack size was large) as shown in (b).

(4) The decrease in n_{ave} with increasing L was, in appearance, similar to that in $I_{c,ave}$ but the extent of the decrease in n_{ave} was severer than that of $I_{c,ave}$, as indicated by the difference between $n_{ave}/n_0 - L$ and $I_{c,ave}/I_{c0} - L$ curves. Namely, specimen length-dependence of n_{ave} was larger than that of $I_{c,ave}$.

3.2 Relation of *V–I* curves of sections to the *V–I* curve, critical current and *n*-value of specimen

Figures 4(a) and 4(b) show two examples (example A1 in (a) and example A2 in (b)) of the simulated *V–I* curves of specimen with a length 7.5 cm, constituted of 5 sections with a length 1.5 cm. These examples were selected from many results as to show the influence of the difference in location of the *V–I* curves among the sections on the I_c- and n-values of specimen. These examples had the following features.

(i) The values of (I_c, n) of sections of example A1 and those of example A2 are listed in the caption of Fig. 4. The average values of ($I_{c,ave}$, n_{ave}) of the sections of example A1 and example A2 were (136 A, 27.6) and (136 A, 28.3), respectively. In both examples, the $I_{c,ave}$ and n_{ave} of the 5 sections were commonly 136 A and ≈28, respectively. On the other hand, positional relation among the *V–I* curves of the sections was quite different between the examples. In the example A1, the *V–I* curves of the sections existed in narrow range of current, and the difference in value of (I_c, n) among the sections was small, corresponding to the case of small difference in crack size among sections. In contrast, in the example A2, the *V–I* curves of the sections existed in wide current range, and hence, the difference in values of (I_c, n) among the sections was large, corresponding to the case of large difference in crack size among sections.

(ii) The values of (I_c, n) of the specimen of example A1 and example A2 were (129 A, 21.9) and (96.0 A, 11.7), respectively. Despite that $I_{c,ave}$ and n_{ave} of sections of example A1 were almost the same as those A2, the (I_c, n)-values of the specimens constituted of the sections were quite different between the examples due to the difference in positional relation among the *V–I* curves of the sections.

(iii) The *V–I* curve of the section with the lowest I_c contributes most largely to the *V–I* curve of the specimen than the *V–I* curves of other sections. This feature became more prominent when the distance between the *V–I* curve of the sections with the lowest and second lowest I_c was larger. It is noted that even though the $I_{c,ave}$- and n_{ave}-values of the sections were almost the same in examples A1 and A2 (Fig. 4(a, b)), both of I_c- and n-values of specimen became lower when the distance among the *V–I* curves of sections was larger, namely when crack size was largely different among the sections. If we assume that difference in crack size among the sections is zero, the I_c- and n-values of all sections are the same as those of specimens. In such an assumed case, the values of (I_c, n) of the specimen with any length are (136 A, 28) in the present examples. In the example A1 where the difference in crack size among sections was small, (I_c, n) values decreased to (129 A, 22), and in the example A2 where it was large, they decreased to (96 A, 12). In this way, I_c and n-value of specimen decrease with increasing difference in crack size among sections even when the average critical current is same.

As shown in Figs. 4(a) and 4(b), the largest crack in the section S(4) played a dominant role in determination of I_c, whether the cracks of the other sections had similar size

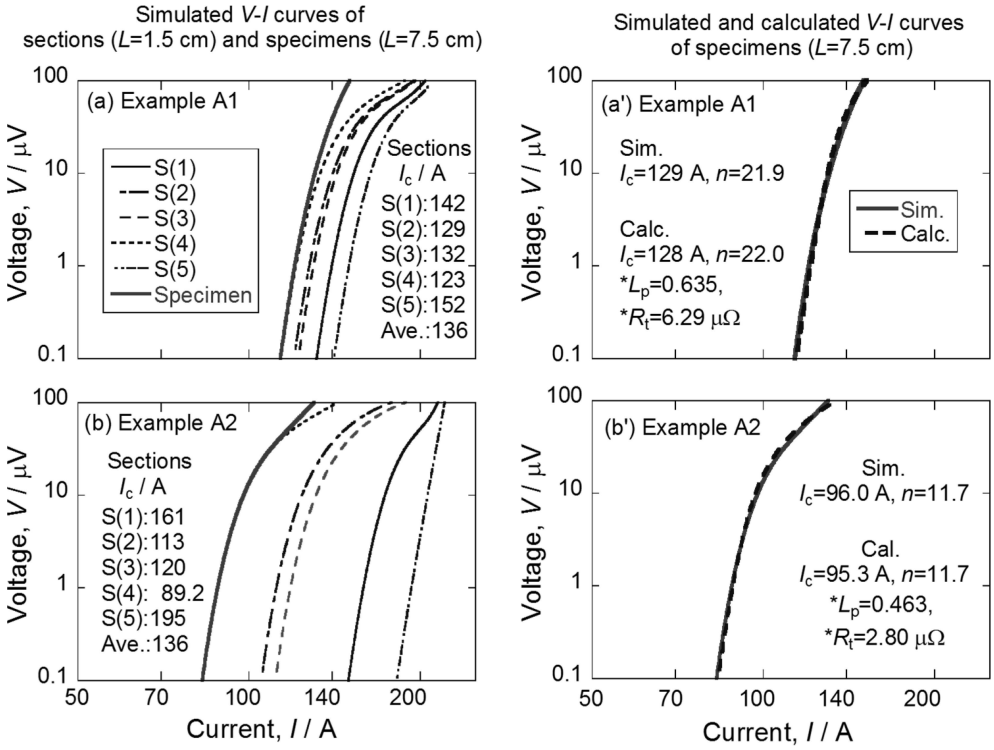

Fig. 4 Examples of (a, b) the distributed *V*–*I* curves of the sections with different crack size and their influence on the *V*–*I* curve of the specimen, and (a', b') the analyzed *V*–*I* curves of the specimens with a single equivalent crack-current shunting model. The *V*–*I* curves are drawn in logarithmic scale for both *V*- and *I*-axial directions. Difference between (a, a') and (b, b') show the influence of distribution width of the *V*–*I* curves of the sections on critical current and *n*-value under the situation where the average critical current of sections are common. The specimen length *L* was 7.5 cm in these examples. The values of (I_c, n) of sections in (a) were S(1);(142 A, 28.0), S(2):(129 A, 27.2), S(3):(132 A, 27.4), S(4):(123 A, 26.8), S(5):(152 A, 28.4) and the those in (b) were S(1);(161 A, 28.8), S(2):(113 A, 25.9), S(3):(120 A, 26.5), S(4):(89.2 A, 23.6), S(5):(195 A, 36.5). The average values of ($I_{c,ave}$, n_{ave}) of the sections in (a) and (b) were (136 A, 27.6) and (136 A, 28.3), respectively.

(Fig. 4(a)) or different size (Fig. 4(b)). However, the *n*-value of specimen was strongly dependent not only on the largest crack but also on the second, third,....., largest cracks; namely *n*-value was dependent on the difference in crack size, which was reflected in the difference of positional relation among the *V*–*I* curves of sections. Figures 5(a) and (b) show the distributed *V*–*I* curves of the sections and their influence on the *V*–*I* curve of the specimens of the example B1 and example B2, respectively. The specimen length *L* was 7.5 cm in these examples. The (I_c, n) values of the specimens of examples B1 and B2 were (123 A, 22.5) and (122 A, 13.6), respectively. The I_c-values of specimens of examples B1 (123 A) and B2 (122 A) were almost the same but the *n*-values of specimens (22.5 (B1) and 13.6 (B2)) were quite different from each other. It is clearly shown that, even though the I_c-values of the two specimens were the same to each other, the *n*-value of one specimen (example B1 in which the *V*–*I* curves of sections exist near to each other, Fig. 5(a)) was higher than the *n*-value of another specimen (example B2 in which the *V*–*I* curve of the section with the largest crack (the lowest I_c) was far away from the *V*–*I* curves of other sections, Fig. 5(b)). This result indicates that the correlation between I_c and *n*-value is not determined uniquely since plural *n*-values can be existent for one I_c-value, depending on the positional relation among the *V*–*I* curves of sections.

3.3 Description of *V*–*I* curve, critical current and *n*-value of specimens containing plural cracks (2 ≤ N) with a single equivalent crack-current shunting model

In analysis of the measured *V*–*I* curve, I_c, and *n*-value of coated- and filamentary conductor tape specimens with stress-induced cracks[3–5,8,10,14,15,21], we have been replacing the multiple cracks with a single equivalent crack in the model, because current shunting occurs via the same mechanism in both single and multiple cracks. Despite the replacement, the experimental results have been described well, suggesting that replacement is a useful analysis tool in practice.

Based on the results stated above, the single equivalent crack-current shunting model was used also in this work for characterization of the simulated *V*–*I* curves of the specimens with a length L = 7.5 cm shown in Fig. 4(a) and 4(b). In application of this model, the unknown values were the ligament parameter L_p for L = 7.5 cm and the electric resistance R_t of current shunting circuit in eqs. (2) and (3). Replacing L_0 (1.5 cm) by L (= 7.5 cm in this case) and setting $L_p = (1 - f)(L/s)^{1/n_0}$ in eqs. (2) and (3), and fitting eqs. (2) and (3) to the simulated *V*–*I* curves, we obtained the unknown values; L_p = 0.635 and R_t = 6.3 $\mu\Omega$ for the specimen of example A1, and L_p = 0.463 and R_t = 2.8 $\mu\Omega$ for the specimen of example A2, as shown in Fig. 4(a') and 4(b'). By substituting the obtained values of L_p and R_t into eqs. (2) and (3), the *V*–*I* curve was back-calculated as shown with broken

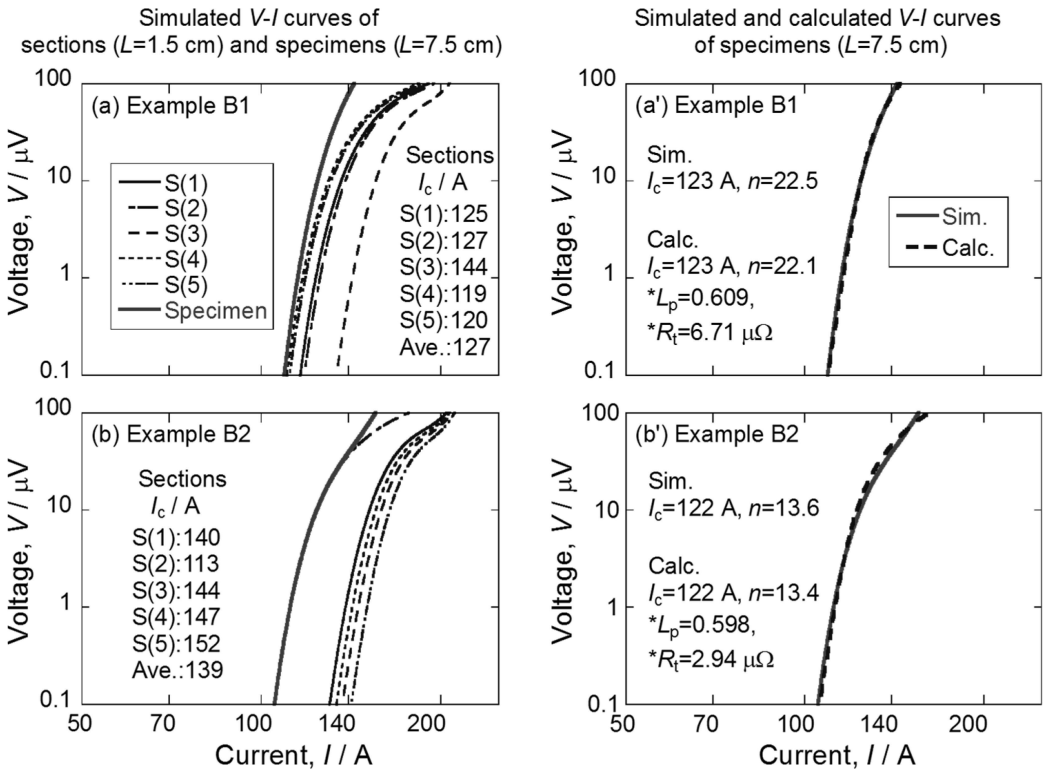

Fig. 5 Examples of (a, b) the distributed *V–I* curves of the sections with different crack size and their influence on the *V–I* curve of the specimen, and (a', b') the analyzed *V–I* curves of the specimens with a single equivalent crack-current shunting model. (a, a') and (b, b') show the cases where critical current of the specimens is almost the same but *n*-value is different due to the difference in positional relation among the *V–I* curves of sections. The specimen length *L* was 7.5 cm in these examples.

curves, describing well the simulated ones. From the back-calculated *V–I* curves, the values of (I_c, n) of specimen of example A1 were estimated to be (128 A, 22). The simulation result of (129 A, 21.9) was well reproduced. In the same way, the values of (I_c, n) of the specimen of example A2 was back-calculated to be (95.3 A, 11.7), reproducing well the simulation result of (96.0 A, 11.7). From these results, it was reconfirmed that the single equivalent crack-current shunting model can be used to describe the *V–I* curve of specimens with multiple cracks via estimation of the values of L_p and R_t.

The *V–I* curves of the specimens of examples B1 and B2 analyzed with the single equivalent crack-current shunting model are shown in Fig. 5(a') and 5(b'), respectively. The *V–I* curve, I_c and *n*-value of the specimens of both examples were reproduced well by this model. The R_t-value for lower *n*-value (example B2) was lower than that for higher *n*-value (example B1). This result means that *n*-value varies with R_t under a given I_c-value, reflecting the positional relation among *V–I* curves of sections; when the *V–I* curves of many sections exist near to the *V–I* curve of the lowest I_c–section (most seriously cracked section) as in Fig. 5(a'), many sections contribute to raise the voltage of the specimen and hence high *n*-value is realized in specimen. In this process, as the specimen is constituted of a series of sections, the resistances in shunting circuit in the sections with the largest, second, third...cracks are summed up, and hence R_t-value of the specimen becomes high. On the other hand, when the *V–I* curve of the section with the largest crack is isolated as in Fig. 5(b), it is equal to the *V–I* curve of the specimen where the other sections do not contribute to the voltage of the specimen. Accordingly *n*-value of the specimen is low. In such a case, current shunting occurs only in one section and hence R_t is low. In this way, the phenomenon, in which different *n*-values were existent for one I_c-value, could be described by the difference of the level of R_t.

3.4 Effects of specimen length and crack size distribution on the correlation between *n*-value and critical current I_c, and description of *n*-I_c correlation diagram

From the pair-values of (I_c, n) of specimens obtained by the Monte Carlo simulation, *n*-value was plotted against I_c-value, and the *n*-I_c correlation diagrams were obtained, as shown in Fig. 6. (a, b, c, d) show the results for the specimen length L = 3, 6, 9 and 15 cm, respectively, under the condition of small distribution width of crack size, monitored by $\Delta L_{p,section}$ = 0.05, and (a', b', c', d') show the results for the specimen length L = 3, 6, 9 and 15 cm, respectively, under the condition of large distribution width of crack size, monitored by and $\Delta L_{p,section}$ = 0.15.

The results shown in subsection 3.2 means that the relation of *n*-value to I_c is not determined uniquely but has some width in the direction of *n*-value for a given I_c-value due to the difference in the positional relation among the *V–I* curves of sections. For description of the *n*-I_c diagram in which *n*-value is not uniquely determined by I_c-value, we estimated the upper-lower bounds and the center of the *n*-I_c correlation by finding R_t-values through the application of the single equivalent crack-current shunting model directly

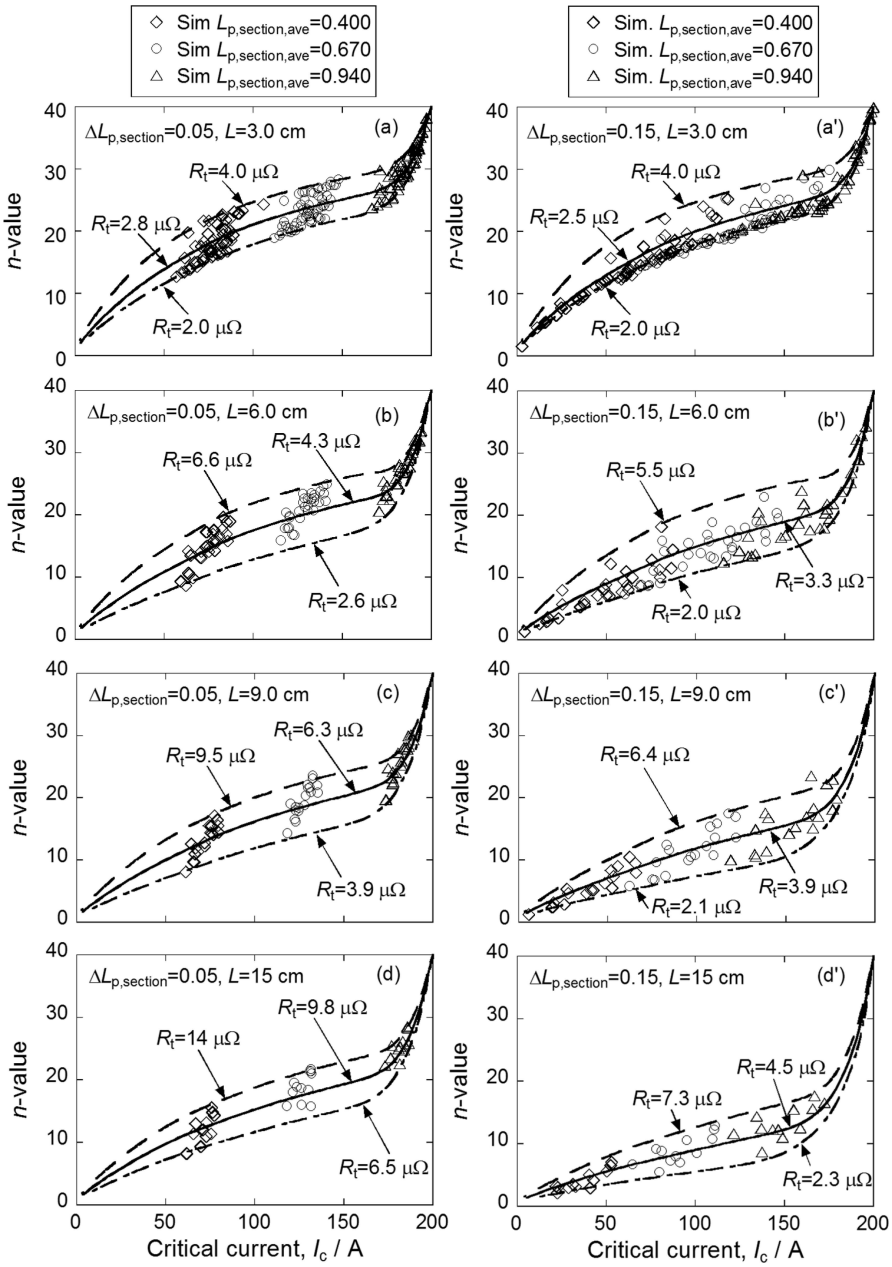

Fig. 6 Description of the n-I_c diagrams by finding the R_t-values for the upper bound (long dashed line), center (solid line) and lower bound (dashed dotted line). (a)~(d) and (a')~(d') show the simulated and analyzed results for $\Delta L_{p,section}$ = 0.05 and 0.15, respectively. (a, a'), (b, b'), (c, c') and (d, d') show the results for L = 3, 6, 9 and 15 cm, respectively.

to the measured n-I_c diagram. Hereafter, this approach is noted simply as the upper-lower bounds approach. In our preceding work[21], we found that the upper-lower bounds approach can describe the experimental results satisfactorily. However, due to the lack of experimental data, the effect of specimen length on the n-I_c diagram was not studied at that time. In this subsection, as a next step, we investigate the effects of the specimen length on the n-I_c diagram.

The results of application of the upper-lower bounds approach to the simulation results of the n-I_c diagram are presented also in Fig. 6, in which the upper bound (long dashed line), the lower bound (broken line) and the center (solid line), together with the corresponding R_t-values, are presented. The following features are read. (a) The n-I_c diagrams for various specimen lengths in both cases of small and large distribution widths of crack size are described by the present upper-lower bounds approach using R_t-value as a parameter. (b) For a given specimen length, the R_t-values giving upper and lower bounds of the n-I_c relation in the case of $\Delta L_{p,section}$ = 0.05 is higher than those in the case of $\Delta L_{p,section}$ = 0.15. The high R_t in the case of $\Delta L_{p,section}$ = 0.05 is attributed to the larger number of sections that contribute to raise V of the specimen since the V–I curves of the sections are near to each other. In the case of $\Delta L_{p,section}$ = 0.15, the interspacing among the V–I curves of the sections is large and the number of the sections that contribute to raise V of the specimen is small, and hence R_t is lower. (c) The number of the sections, whose V–I curves are near to the V–I curve of the largest crack-section, increases, and hence R_t-value increases, too, with increasing specimen length. (d)

While the R_t values both for upper and lower bounds increase with increasing L, the extent of increase in R_t with specimen length was quite different between the cases of small and large difference in crack size among the sections. The value of R_t increases with specimen length more intensively when the difference in crack size among the sections is smaller.

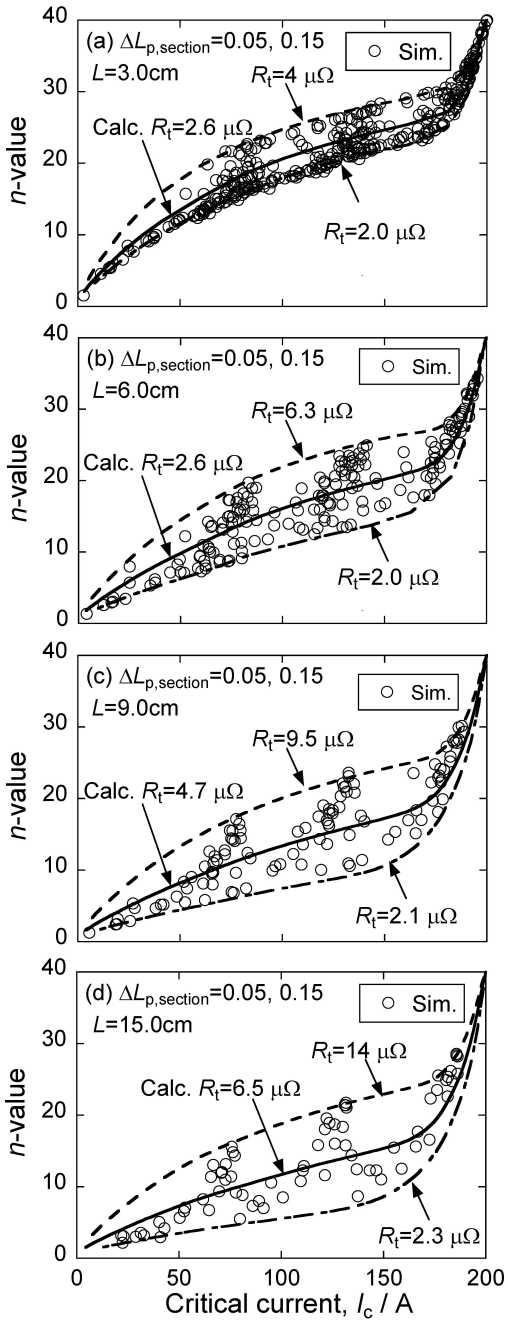

Fig. 7 Description of the n-I_c diagrams, in which simulated data both for $\Delta L_{p,section}$ = 0.05 and 0.15 are included together as to monitor the practical situation where the standard deviation of crack size vary widely under applied stress to specimens. (a), (b), (c) and (d) show the results for L = 3, 6, 9 and 15 cm. The R_t-values to describe the upper bound (short dashed line), center (solid line) and lower bound (dashed dotted line) in the n-I_c diagram are indicated in (a) to (d).

3.5 Application of the upper-lower bounds approach to description of the specimen length-dependence of the n-I_c diagram

When stress is exerted on the tape, the situation of cracking is complex. Both of large and small distribution widths of crack size arise with varying stress level; in some case, the distribution width of crack size increases monotonically with increasing stress, in some case, it increases and then decreases, and in some case, it increases and decreases alternatively. For description of measured n-I_c correlation diagram for wide range of I_c, it is required to incorporate both cases of large and small distribution widths of crack size.

In order to monitor such a practical situation, we included both cases of large ($\Delta L_{p.section}$ = 0.15) and small ($\Delta L_{p.section}$ = 0.05) standard deviation of crack size together, and analyzed with the upper-lower bounds approach. The results are shown in Fig. 7. In this case, the upper bound was the same as the upper bound for $\Delta L_{p.section}$ = 0.05 and the lower bound was the same as the lower bound for $\Delta L_{p.section}$ = 0.15. For all specimen lengths (3–30 cm in this work), the upper-lower bounds and the center of the n-I_c correlation diagrams were described successfully by this approach.

Under the actually occurring situation where both cases of

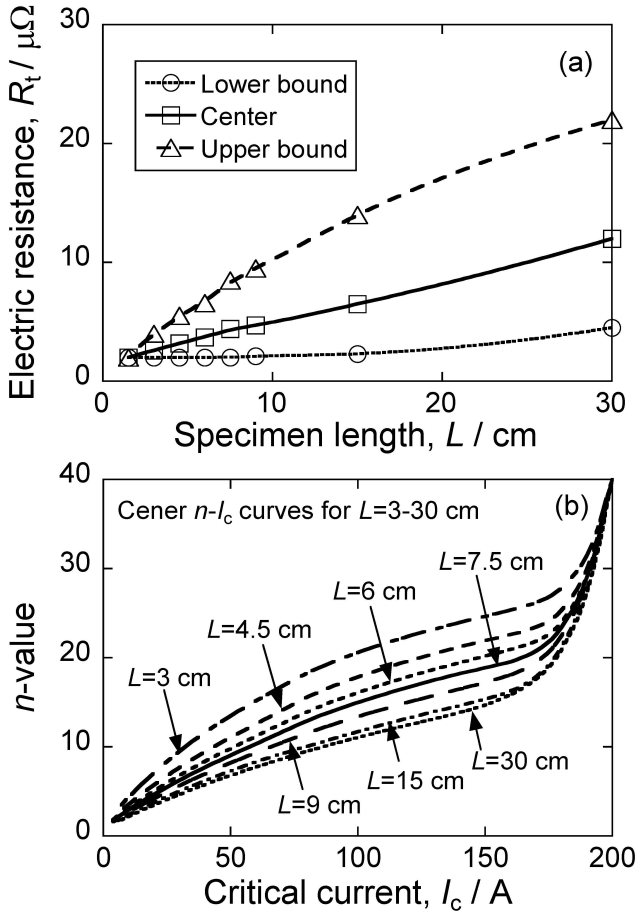

Fig. 8 (a) Change in R_t-value with increasing specimen length L for the upper-lower bounds and the center. (b) Change in the n-I_c relation of the center in the n-I_c diagram with increasing L, calculated with the R_t-values shown in (a) (R_t = 2.6, 3.2, 3.7, 4.4, 4.7, 6.5 and 12.0 $\mu\Omega$ for L = 3, 4.5, 6. 7.5, 9, 15 and 30 cm, respectively). In (b), In (b), the n-I_c curves for the center are taken up representatively from the n-I_c curves calculated for the upper-lower bounds and the center.

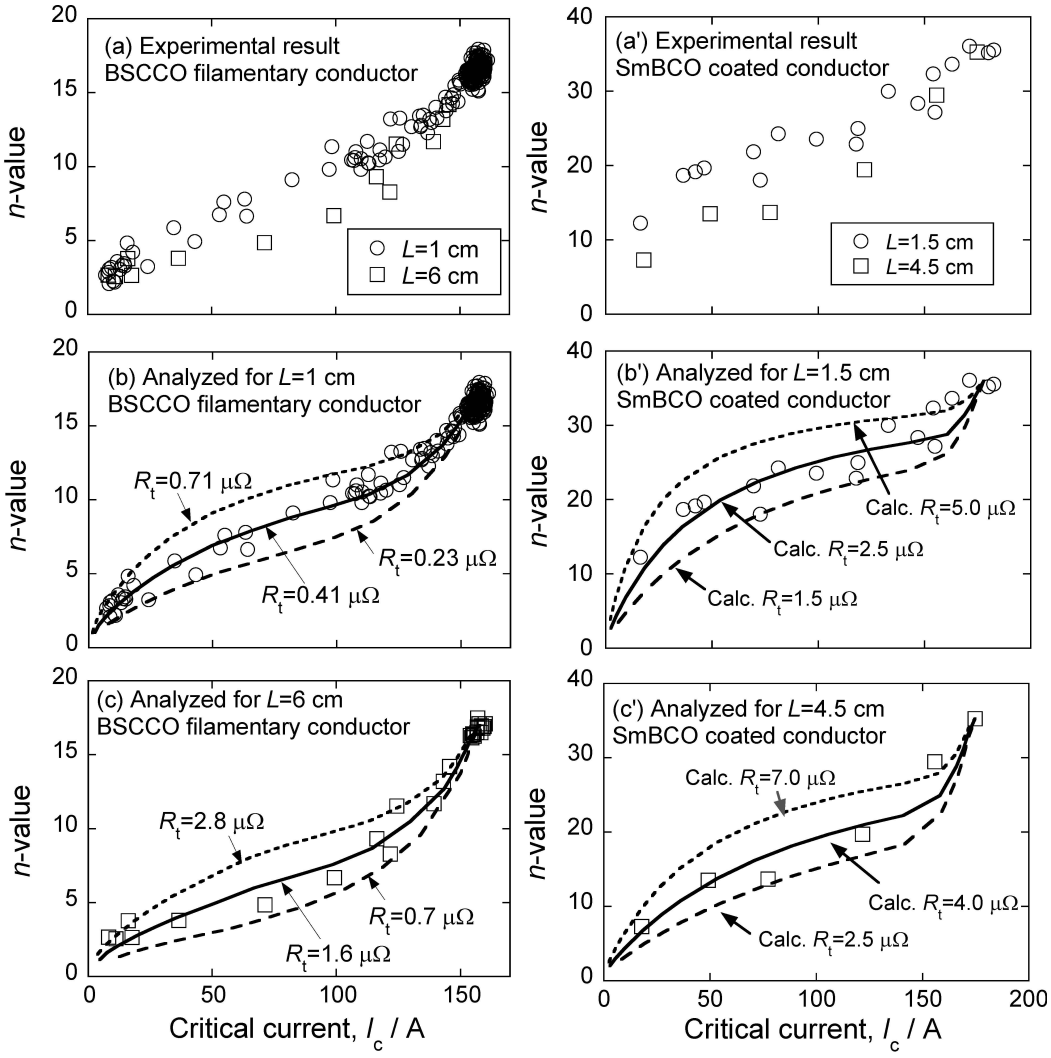

Fig. 9 Examples of specimen length-dependence of experimentally measured *n*-I_c diagrams and the results analyzed by the upper-lower bounds approach for filamentary- and coated- conductor tapes. (a) and (a') show the experimental results of BSCCO filamentary tape for L = 1 cm and 6 cm[15] and SmBCO coated tape for L = 1.5 cm and 4.5 cm[8], respectively. (b) and (c) show the analyzed results of BSCCO filamentary tape for L = 1 cm and 6 cm, respectively. (b') and (c') show the analyzed results of SmBCO coated tape for L = 1.5 cm and 4.5 cm, respectively.

small and large difference in crack size co-exist, the change in R_t-value with increasing specimen length L for the upper-lower bounds and the center, was obtained, as shown in Fig. 8(a). The R_t for all of the upper-lower bounds and the center increased with L, but the extent of the increase of R_t with L was different; it was high at the upper bound, low at the lower bound and intermediate at the center. Using the R_t-value obtained for each length, the change in *n*-I_c relation with L for the upper-lower bounds and the center was calculated. As a representative, the change in *n*-I_c relation of the center in *n*-I_c diagram is shown in Fig. 8(b). The experimentally observed feature that *n*-I_c curve tends to shift to lower *n*-range with increasing specimen length was reproduced well.

The results shown in Figs. 6 and 7 indicate that the *n*-I_c diagram for any specimen length and for any standard deviation of crack size can be described by the upper-lower bounds approach using a single equivalent crack-current shunting model. Based on this result, the present approach was applied to the experimentally measured specimen length- dependent *n*-I_c diagrams of filamentary BSCCO tape[21] and SmBCO coated tape[10]. The results are shown in Fig. 9. The experimentally measured *n*-I_c diagrams of both (a, b, c) BSCCO filamentary conductor tape with L = 1 cm and 6 cm and (a', b', c') SmBCO coated conductor tape with L = 1.5 cm and 4.5 cm were well described by the present approach.

In this way, we can describe the experimental results of the specimen length-dependence of the *n*-I_c diagram by estimating the upper-lower bounds and the center with the single equivalent crack-current shunting model. This approach is simple and is practically a useful tool for describing specimen length-dependence of *n*-I_c diagrams both of filamentary and coated conductors.

4. Conclusions

(1) In any specimen length, the distributions of both critical current I_c- and *n*-values became wider, and average I_c- and *n*-values became lower when the crack size distribution was wider. The extent of decrease with increasing distribution width of crack size was different between

average I_c- and n-values; the average n-value became lower more intensively than the average I_c-value.

(2) Both of average I_c-value and average n-value decreased with increase in specimen length under a given crack size distribution. This phenomenon was more remarkable when crack size distribution was wider. The extent of decrease with increase in specimen length was different between I_c and n-value; n-value decreased more sensitively to specimen length than the I_c-value.

(3) The n-value of specimen was dependent on the positional relation among the voltage-current curves of the sections, of which specimen was constituted. The voltage-current curve of the section having the lowest I_c-value (having the largest crack) was located in the low current side than the voltage-current curves of other sections. When the voltage-current curves of the other sections having higher I_c-values (having smaller cracks), were dense and coarse in the neighborhood of the voltage-current curve of the section having the lowest I_c-value, high and low n-values arose in specimen, respectively. Thus plural n-values could be existent for an I_c-value of specimen. This results indicate that the n-I_c relation is not described uniquely in heterogeneously cracked specimens. The upper-lower bounds approach is useful for description.

(4) The simulated V–I curve, I_c and n-value of specimens with plural cracks could be described by using the single equivalent crack-current shunting model, in which plural cracks are replaced by a single equivalent crack. In this model, the resistance R_t-value in shunting circuit reflects the situation of interspacing among the V–I curves of sections and hence effective number of sections that contribute to synthesize the V–I curve of the specimen.

(5) The n-I_c diagrams obtained by the simulation at various specimen lengths and the n-I_c diagrams of the filamentary- and coated- conductor tapes measured experimentally for different specimen lengths were described by estimating R_t-values with the single equivalent crack-current shunting model for the upper-lower bounds and the center of the n-I_c correlation diagram

REFERENCES

1) K. Osamura, M. Sugano, S. Machiya, H. Adachi, S. Ochiai and M. Sato: Supercond. Sci. Technol. **22** (2009) 065001.
2) D.C. van der Laan, J.W. Ekin, F.F. Douglas, C.C. Clickner, T.C. Stauffer and L.F. Goodrich: Supercond. Sci. Technol. **23** (2010) 072001.
3) S. Ochiai, T. Arai, A. Toda, H. Okuda, M. Sugano, K. Osamura and W. Prusseit: J. Appl. Phys. **108** (2010) 063905.
4) S. Ochiai, H. Okuda, T. Arai, S. Nagano, M. Sugano and W. Prusseit: Cryogenics **51** (2011) 584–590.
5) S. Ochiai, H. Okuda, T. Arai, M. Sugano, K. Osamura and W. Prusseit: J. Japan Inst. Copper, Copper and Copper Alloys **52** (2013) 225–230.
6) H.-S. Shin, J. Marlon, H. Dedicatoria, H.-S. Kim, N.-J. Lee, H.-S. Ha and S.-S. Oh: IEEE Trans. Appl. Supercond. **21** (2011) 2997–3000.
7) H. Oguro, T. Suwa, T. Suzuki, S. Awaji, K. Watanabe, M. Sugano, S. Machiya, M. Sato, T. Koganezawa, T. Machi, M. Yoshizumi and T. Izumi: IEEE Trans. Appl. Supercond. **23** (2013) 8400304.
8) S. Ochiai, H. Okuda, M. Sugano, S.-S. Oh and H.-S. Ha: Mater. Trans. **55** (2014) 549–555.
9) S. Ochiai, H. Okuda and N. Fujii: Mater. Trans. **55** (2014) 1479–1487.
10) S. Ochiai, H. Okuda and N. Fujii: Mater. Trans. **56** (2015) 381–388.
11) J.K. Shin, S. Ochiai, H. Okuda, M. Sugano and S.-S. Oh: Supercond. Sci. Technol. **21** (2008) 115007.
12) S. Ochiai, M. Fujimoto, J.K. Shin, H. Okuda, S.S. Oh and D.W. Ha: J. Appl. Phys. **106** (2009) 103916.
13) Y. Fang, S. Danyluk and M.T. Lanagan: Cryogenics **36** (1996) 957–962.
14) S. Ochiai, H. Okuda, M. Sugano, K. Osamura, A. Otto and A.P. Malozemoff: Mater. Trans. **53** (2012) 1549–1555.
15) S. Ochiai, H. Okuda, H. Matsubayashi, K. Osamura and A. Otto: Mater. Trans. **57** (2016) 709–715.
16) N. Banno, D. Uglietti, B. Seeber, T. Takeuchi and R. Flükiger: Supercond. Sci. Technol. **18** (2005) 284–288.
17) Y. Miyoshi, E.P.A. Van Lanen, M.M. Dhalléand and N. Nijhuits: Supercond. Sci. Technol. **22** (2009) 085009.
18) H. Kitaguchi, H. Kumakura and K. Togano: Physica C **363** (2001) 198–201.
19) H. Kitaguchi, A. Matsumoto, H. Hatakeyama and H. Kumakura: Physica C **401** (2004) 246–250.
20) S. Ochiai, H. Okuda and N. Fujii: Mater. Trans. **58** (2017) 679–687.
21) S. Ochiai, H. Okuda, M. Fujimoto and K. Osamura: Mater. Trans. **56** (2015) 1558–1564.